

2022 Update on ε_K with lattice QCD inputs

Sunghee Kim,^{a,1} Sunkyuu Lee,^{a,1} Weonjong Lee,^{a,b,1,*} Jaehoon Leem^{b,c,1} and Sungwoo Park^{d,1}

^aLattice Gauge Theory Research Center, CTP, and FPRD, Department of Physics and Astronomy, Seoul National University, Seoul 08826, South Korea

^bSchool of Physics, Korea Institute for Advanced Study (KIAS), Seoul 02455, South Korea

^cComputational Science and Engineering Team, Innovation Center, Samsung Electronics, Hwaseong, Gyeonggi-do 18448, South Korea.

^dThomas Jefferson National Accelerator Facility, 12000 Jefferson Avenue, Newport News, VA 23606, USA

E-mail: wlee@snu.ac.kr

We present recent updates for ε_K determined directly from the standard model (SM) with lattice QCD inputs such as \hat{B}_K , $|V_{cb}|$, $|V_{us}|$, ξ_0 , ξ_2 , ξ_{LD} , f_K , and m_c . We find that the standard model with exclusive $|V_{cb}|$ and other lattice QCD inputs describes only 65% of the experimental value of $|\varepsilon_K|$ and does not explain its remaining 35%, which leads to a strong tension in $|\varepsilon_K|$ at the $5.1\sigma \sim 3.9\sigma$ level between the SM theory and experiment. We also find that this tension disappears when we use the inclusive value of $|V_{cb}|$ obtained using the heavy quark expansion based on the QCD sum rule approach, although this inclusive tension is small ($\approx 1.4\sigma$) but keeps increasing as time goes on.

*The 39th International Symposium on Lattice Field Theory,
8th-13th August, 2022,
Rheinische Friedrich-Wilhelms-Universität Bonn, Bonn, Germany*

¹The SWME collaboration

*Speaker

1. Introduction

This paper is an update from our previous reports [1–7]. Here, we present recent progress in determination of $|\varepsilon_K|$ with updated inputs from lattice QCD. Updated input parameters include $\bar{\rho}$, $\bar{\eta}$, exclusive $|V_{cb}|$, inclusive $|V_{cb}|$, M_W , and M_t .

Here, we follow the color convention of our previous papers [1–7] in Tables 1–8. We use the red color for the new input data which is used to evaluate ε_K . We use the blue color for the new input data which is not used for some obvious reason.

2. Input parameters: Wolfenstein parameters

In Table 1 (a), we present the most updated Wolfenstein parameters available in the market. As explained in Ref. [3, 7], we use the results of angle-only-fit (AOF) in Table 1 (a) in order to avoid unwanted correlation between $(\varepsilon_K, |V_{cb}|)$, and $(\bar{\rho}, \bar{\eta})$. We determine λ from $|V_{us}|$ which is obtained from the $K_{\ell 2}$ and $K_{\ell 3}$ decays using lattice QCD inputs for form factors and decay constants as explained in Ref. [8]. We determine the A parameter from $|V_{cb}|$.

| WP | CKMfitter | UTfit | AOF | Input | Value | Ref. |
|--------------|-----------------|-------------------|----------------|-------------|------------|------|
| λ | 0.22475(25) [9] | 0.22500(100) [10] | 0.2249(5) [8] | η_{cc} | 1.72(27) | [4] |
| $\bar{\rho}$ | 0.1577(96) [9] | 0.148(13) [10] | 0.156(17) [11] | η_{tt} | 0.5765(65) | [12] |
| $\bar{\eta}$ | 0.3493(95) [9] | 0.348(10) [10] | 0.334(12) [11] | η_{ct} | 0.496(47) | [13] |

(a) Wolfenstein parameters

(b) η_{ij}

Table 1: (a) Wolfenstein parameters and (b) QCD corrections: η_{ij} with $i, j = c, t$.

3. Input parameters: $|V_{cb}|$

In Table 2 (a) and (b), we present recently updated results for exclusive $|V_{cb}|$ and inclusive $|V_{cb}|$ respectively. In Table 2 (a), we summarize results for exclusive $|V_{cb}|$ obtained by various groups: HFLAV, BELLE, BABAR, FNAL/MILC, LHCb, and FLAG. Results from LHCb comes from analysis on $B_s \rightarrow D_s^* \ell \bar{\nu}$ decays which are not available in the B -factories. Since results for B_s decay channels have poor statistics, we drop out them here without loss of fairness. The rest of results for exclusive $|V_{cb}|$ have comparable size of errors and are consistent with one another within 1.0σ . In addition, we find that the results are consistent between the CLN and BGL analysis, after the clamorous debates [3, 14].

In Table 2 (b), we present recent results for inclusive $|V_{cb}|$. The Gambino group has reported updated results for inclusive $|V_{cb}|$ in 2021. There are a number of attempts to calculate inclusive $|V_{cb}|$ in lattice QCD, but they belong to a category of exploratory study rather than that of precision measurement yet [15].

| channel | value | method | ref | source |
|--|----------------|--------|-----------------|----------------|
| ex-comb | 39.25(56) | CLN | [16] p115e223 | HFLAV-2021 |
| $B \rightarrow D^* \ell \bar{\nu}$ | 39.0(2)(6)(6) | CLN | [17] erratum p4 | BELLE-2021 |
| $B \rightarrow D^* \ell \bar{\nu}$ | 38.9(3)(7)(6) | BGL | [17] erratum p4 | BELLE 2021 |
| $B \rightarrow D^* \ell \bar{\nu}$ | 38.40(84) | CLN | [18] p5t2 | BABAR-2019 |
| $B \rightarrow D^* \ell \bar{\nu}$ | 38.36(90) | BGL | [18] p5t1 | BABAR-2019 |
| $B \rightarrow D^* \ell \bar{\nu}$ | 38.40(78) | BGL | [14] p27e76 | FNAL/MILC-2022 |
| $B_s \rightarrow D_s^* \ell \bar{\nu}$ | 41.4(6)(9)(12) | CLN | [19] p15 | LHCb-2020 |
| $B_s \rightarrow D_s^* \ell \bar{\nu}$ | 42.3(8)(9)(12) | BGL | [19] p15 | LHCb-2020 |
| ex-comb | 39.48(68) | comb | [8] p145 | FLAG-2021 |

(a) Exclusive $|V_{cb}|$ in units of 10^{-3} .

| channel | value | ref | source |
|----------------|-----------|---------------|--------------|
| kinetic scheme | 42.16(51) | [20] p1 | Gambino-2021 |
| kinetic scheme | 42.00(64) | [8, 21] p145 | FLAG-2021 |
| 1S scheme | 41.98(45) | [16] p110e208 | HFLAV-2021 |

(b) Inclusive $|V_{cb}|$ in units of 10^{-3} .

Table 2: Results for (a) exclusive $|V_{cb}|$ and (b) inclusive $|V_{cb}|$. The p115e223 is an abbreviation for Eq. (223) in page 115. The p5t2 is an abbreviation for Table 2 in page 5.

4. Input parameter ξ_0

The absorptive part of long distance effects on ε_K is parametrized into ξ_0 .

$$\xi_0 = \frac{\text{Im } A_0}{\text{Re } A_0}, \quad \xi_2 = \frac{\text{Im } A_2}{\text{Re } A_2}, \quad \text{Re} \left(\frac{\varepsilon'}{\varepsilon} \right) = \frac{\omega}{\sqrt{2}|\varepsilon_K|} (\xi_2 - \xi_0). \quad (1)$$

There are two independent methods to determine ξ_0 in lattice QCD: the indirect and direct methods. The indirect method is to determine ξ_0 using Eq. (1) with lattice QCD results for ξ_2 combined with experimental results for ε'/ε , ε_K , and ω . The direct method is to determine ξ_0 directly using the lattice QCD results for $\text{Im } A_0$, combined with experimental results for $\text{Re } A_0$.

In Table 3 (a), we summarize experimental results for $\text{Re } A_0$ and $\text{Re } A_2$. In Table 3 (b), we summarize lattice results for $\text{Im } A_0$ and $\text{Im } A_2$ calculated by RBC-UKQCD. In Table 3 (c), we summarize results for ξ_0 which is obtained using results in Table 3 (a) and (b).

Here, we use results of the indirect method for ξ_0 to evaluate ε_K , since its systematic and statistical errors are much smaller than those of the direct method.

5. Input parameters: \hat{B}_K , ξ_{LD} , and others

In FLAG 2021 [8], they report lattice QCD results for \hat{B}_K with $N_f = 2$, $N_f = 2 + 1$, and $N_f = 2 + 1 + 1$. Here, we use the results for \hat{B}_K with $N_f = 2 + 1$, which is obtained by taking an

| parameter | method | value | Ref. | source |
|-----------------------------------|--------|---------------------------------|----------|----------|
| Re A_0 | exp | $3.3201(18) \times 10^{-7}$ GeV | [22, 23] | NA |
| Re A_2 | exp | $1.4787(31) \times 10^{-8}$ GeV | [22] | NA |
| ω | exp | 0.04454(12) | [22] | NA |
| $ \varepsilon_K $ | exp | $2.228(11) \times 10^{-3}$ | [24] | PDG-2021 |
| Re (ε'/ε) | exp | $1.66(23) \times 10^{-3}$ | [24] | PDG-2021 |

(a) Experimental results for ω , Re A_0 and Re A_2 .

| parameter | method | value (GeV) | Ref. | source |
|-----------|---------|----------------------------------|-------------|-------------|
| Im A_0 | lattice | $-6.98(62)(144) \times 10^{-11}$ | [25] p4t1 | RBC-UK-2020 |
| Im A_2 | lattice | $-8.34(103) \times 10^{-13}$ | [25] p31e90 | RBC-UK-2020 |

(b) Results for Im A_0 , and Im A_2 in lattice QCD.

| parameter | method | value | ref | source |
|-----------|----------|------------------------------|------|--------|
| ξ_0 | indirect | $-1.738(177) \times 10^{-4}$ | [25] | SWME |
| ξ_0 | direct | $-2.102(472) \times 10^{-4}$ | [25] | SWME |

(c) Results for ξ_0 obtained using the direct and indirect methods in lattice QCD.

Table 3: Results for ξ_0 . Here, we use the same notation as in Table 2.

average over the four data points from BMW 11, Laiho 11, RBC-UKQCD 14, and SWME 15 in Table 4 (a).

| Collaboration | Ref. | \hat{B}_K | Input | Value | Ref. |
|---------------|------|-----------------|--------------|---|-------------|
| SWME 15 | [26] | 0.735(5)(36) | G_F | $1.1663787(6) \times 10^{-5}$ GeV ⁻² | PDG-22 [30] |
| RBC/UKQCD 14 | [27] | 0.7499(24)(150) | M_W | 80.356(6) GeV | SM-22 [30] |
| Laiho 11 | [28] | 0.7628(38)(205) | θ | 43.52(5) ^o | PDG-22 [30] |
| BMW 11 | [29] | 0.7727(81)(84) | m_{K^0} | 497.611(13) MeV | PDG-22 [30] |
| FLAG 2021 | [8] | 0.7625(97) | ΔM_K | $3.484(6) \times 10^{-12}$ MeV | PDG-22 [30] |
| | | | F_K | 155.7(3) MeV | FLAG-21 [8] |

(a) \hat{B}_K

(b) Other parameters

Table 4: (a) Results for \hat{B}_K and (b) other input parameters.

The dispersive long distance (LD) effect is defined as

$$\xi_{LD} = \frac{m'_{LD}}{\sqrt{2}\Delta M_K}, \quad m'_{LD} = -\text{Im} \left[\mathcal{P} \sum_C \frac{\langle \bar{K}^0 | H_w | C \rangle \langle C | H_w | K^0 \rangle}{m_{K^0} - E_C} \right] \quad (2)$$

As explained in Refs. [3], there are two independent methods to estimate ξ_{LD} : one is the BGI estimate [31], and the other is the RBC-UKQCD estimate [32, 33]. The BGI method is to estimate

| Collaboration | N_f | $m_c(m_c)$ | Ref. | Collaboration | M_t | $m_t(m_t)$ | Ref. |
|---------------|-----------|------------|------|---------------|------------|----------------|------|
| FLAG 2021 | 2 + 1 | 1.275(5) | [8] | PDG 2019 | 172.9(4) | 163.08(38)(17) | [35] |
| FLAG 2021 | 2 + 1 + 1 | 1.278(13) | [8] | PDG 2021 | 172.76(30) | 162.96(28)(17) | [24] |
| | | | | PDG 2022 | 172.69(30) | 162.90(28)(17) | [30] |

(a) $m_c(m_c)$ [GeV] (b) $m_t(m_t)$ [GeV]

Table 5: Results for (a) charm quark mass and (b) top quark mass.

the size of ξ_{LD} using chiral perturbation theory as follows,

$$\xi_{LD} = -0.4(3) \times \frac{\xi_0}{\sqrt{2}} \tag{3}$$

The RBC-UKQCD method is to estimate the size of ξ_{LD} as follows,

$$\xi_{LD} = (0 \pm 1.6)\% \tag{4}$$

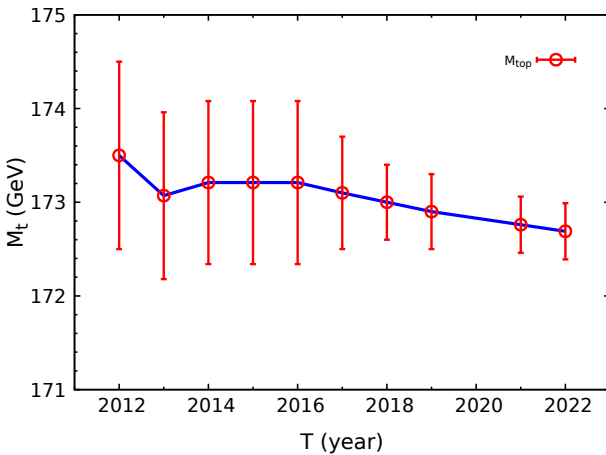
Here, we use both methods to estimate the size of ξ_{LD} .

In Table 1 (b), we present higher order QCD corrections: η_{ij} with $i, j = t, c$. A new approach using $u - t$ unitarity instead of $c - t$ unitarity appeared in Ref. [34], which is supposed to have a better convergence with respect to the charm quark mass. But we have not incorporated this into our analysis yet, which we will do in near future.

In Table 4 (b), we present other input parameters needed to evaluate ε_K .

6. Quark masses

In Table 5, we present the charm quark mass $m_c(m_c)$ and top quark mass $m_t(m_t)$. From FLAG 2021 [8], we take the results for $m_c(m_c)$ with $N_f = 2 + 1$, since there is some inconsistency among the lattice results of various groups with $N_f = 2 + 1 + 1$. For the top quark mass, we use the PDG 2022 results for the pole mass M_t to obtain $m_t(m_t)$.

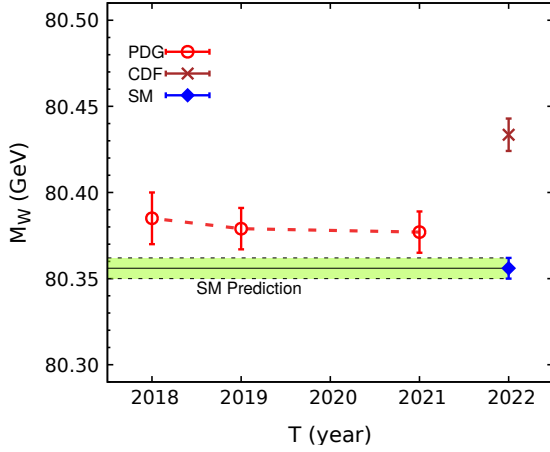


(a) History of M_t (top quark pole mass).

| source | error (%) | memo |
|--------------|-----------|-------------|
| $ V_{cb} $ | 49.7 | Exclusive |
| η_{ct} | 20.7 | $c - t$ Box |
| $\bar{\eta}$ | 13.3 | AOF |
| η_{cc} | 8.7 | $c - c$ Box |
| ξ_{LD} | 2.1 | RBC-UKQCD |
| $\bar{\rho}$ | 2.1 | AOF |
| \hat{B}_K | 1.7 | FLAG |
| \vdots | \vdots | \vdots |

(b) Error budget for $|\varepsilon_K|^{SM}$

Table 6: (a) M_t history (b) error budget.



(a) History of M_W (W boson mass).

| Source | M_W (GeV) | Ref. |
|----------|-------------|------|
| SM-2022 | 80.356(6) | [30] |
| CDF-2022 | 80.4335(94) | [36] |
| PDG-2021 | 80.377(12) | [24] |
| PDG-2019 | 80.379(12) | [35] |
| PDG-2018 | 80.385(15) | [37] |

(b) Table of M_W

Table 7: (a) M_W history (b) table of M_W .

In Table 6 (a), we plot top pole mass M_t as a function of time. Here we find that the average value drifts downward a little bit and the error shrinks fast as time goes on, thanks to accumulation of high statistics in the LHC experiments. The data for 2020 is dropped out intentionally to reflect on the absence of Lattice 2020 due to COVID-19.

7. W boson mass

In Fig. 7 (a), we plot M_W (W boson mass) as a function of time. The corresponding results for M_W are summarized in Table 7 (b). In Fig. 7 (a), the light-green band represents the standard model (SM) prediction, the red circles represents the PDG results, and the brown cross represents the CDF-2022 result. The upside is that the CDF-2022 result is the most precise and latest experimental result for M_W . The downside, however, is that it has a 6.9σ tension from that of SM-2022 (the standard model prediction). Here, we use the SM-2022 result for M_W to evaluate ε_K .

8. Results for ε_K

In Fig. 1, we show results for $|\varepsilon_K|$ evaluated directly from the standard model (SM) with lattice QCD inputs given in the previous sections. In Fig. 1 (a), the blue curve represents the theoretical evaluation of $|\varepsilon_K|$ obtained using the FLAG-2021 results for \hat{B}_K , AOF for Wolfenstein parameters, the [FNAL/MILC 2022, BGL] results for exclusive $|V_{cb}|$, results for ξ_0 with the indirect method, and the RBC-UKQCD estimate for ξ_{LD} . The red curve in Fig. 1 represents the experimental results for $|\varepsilon_K|$. In Fig. 1 (b), the blue curve represents the same as in Fig. 1 (a) except for using the 1S scheme results for the inclusive $|V_{cb}|$.

Our results for $|\varepsilon_K|^{\text{SM}}$ and $\Delta\varepsilon_K$ are summarized in Table 8. Here, the superscript $^{\text{SM}}$ represents the theoretical expectation value of $|\varepsilon_K|$ obtained directly from the SM. The superscript $^{\text{Exp}}$ represents the experimental value of $|\varepsilon_K| = 2.228(11) \times 10^{-3}$. Results in Table 8 (a) are obtained using the RBC-UKQCD estimate for ξ_{LD} , and those in Table 8 (b) are obtained using the BGI estimate for ξ_{LD} . In Table 8 (a), we find that the theoretical expectation values of $|\varepsilon_K|^{\text{SM}}$ with lattice QCD

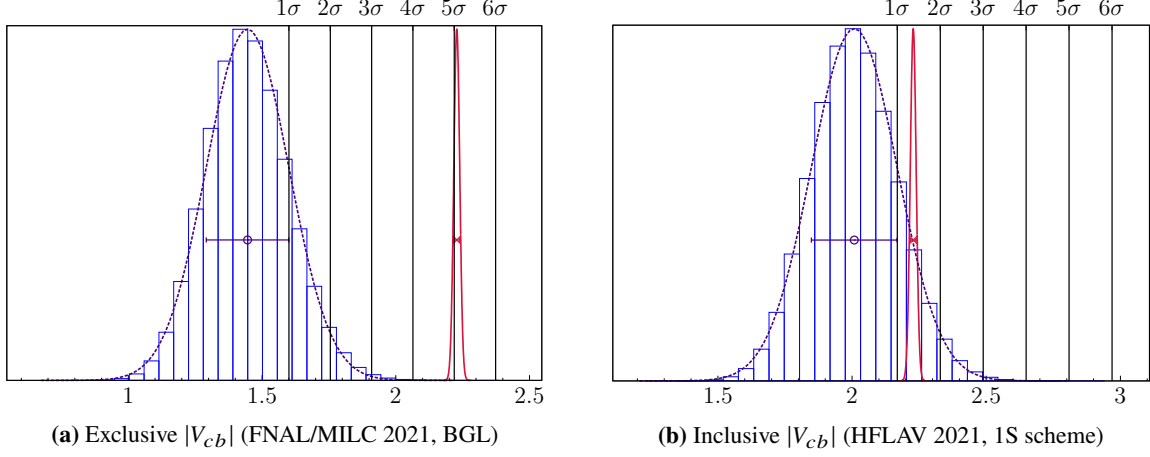


Figure 1: $|\varepsilon_K|$ with (a) exclusive $|V_{cb}|$ (left) and (b) inclusive $|V_{cb}|$ (right) in units of 1.0×10^{-3} .

inputs (with exclusive $|V_{cb}|$) has $5.12\sigma \sim 3.93\sigma$ tension with the experimental value of $|\varepsilon_K|^{\text{Exp}}$, while there is no tension with inclusive $|V_{cb}|$ (obtained using heavy quark expansion and QCD sum rules). We also find that the tension with inclusive $|V_{cb}|$ is small but keeps increasing with respect to time.

In Fig. 2 (a), we show the time evolution of $\Delta\varepsilon_K$ starting from 2012 till 2022. In 2012, $\Delta\varepsilon_K$ was 2.5σ , but now it is 5.05σ with exclusive $|V_{cb}|$ (FNAL/MILC-2022, BGL).¹ In Fig. 2 (b), we

¹Here, we use the results for exclusive $|V_{cb}|$ from FNAL/MILC-2022, since it contains the most comprehensive analysis on the $\bar{B} \rightarrow D^* \ell \bar{\nu}$ decays on both zero recoil and non-zero recoil data points, while it covers both BELL and

| $ V_{cb} $ | method | reference | $ \varepsilon_K ^{\text{SM}}$ | $\Delta\varepsilon_K$ |
|------------|---------|----------------|-------------------------------|-----------------------|
| exclusive | BGL | BELLE 2021 | 1.518 ± 0.180 | 3.93σ |
| exclusive | CLN | BELLE 2021 | 1.532 ± 0.171 | 4.07σ |
| exclusive | BGL | BABAR 2019 | 1.441 ± 0.166 | 4.72σ |
| exclusive | CLN | BABAR 2019 | 1.446 ± 0.161 | 4.86σ |
| exclusive | BGL | FNAL/MILC 2021 | 1.446 ± 0.154 | 5.05σ |
| exclusive | CLN | HFLAV 2021 | 1.566 ± 0.142 | 4.63σ |
| inclusive | kinetic | Gambino 2021 | 2.041 ± 0.168 | 1.12σ |
| inclusive | 1S | HFLAV 2021 | 2.008 ± 0.160 | 1.37σ |

(a) RBC-UKQCD estimate for ξ_{LD}

| $ V_{cb} $ | method | reference | $ \varepsilon_K ^{\text{SM}}$ | $\Delta\varepsilon_K$ |
|------------|--------|----------------|-------------------------------|-----------------------|
| exclusive | BGL | FNAL/MILC 2021 | 1.494 ± 0.157 | 4.66σ |
| exclusive | CLN | HFLAV 2021 | 1.614 ± 0.145 | 4.22σ |

(b) BGI estimate for ξ_{LD}

Table 8: $|\varepsilon_K|$ in units of 1.0×10^{-3} , and $\Delta\varepsilon_K = |\varepsilon_K|^{\text{Exp}} - |\varepsilon_K|^{\text{SM}}$.

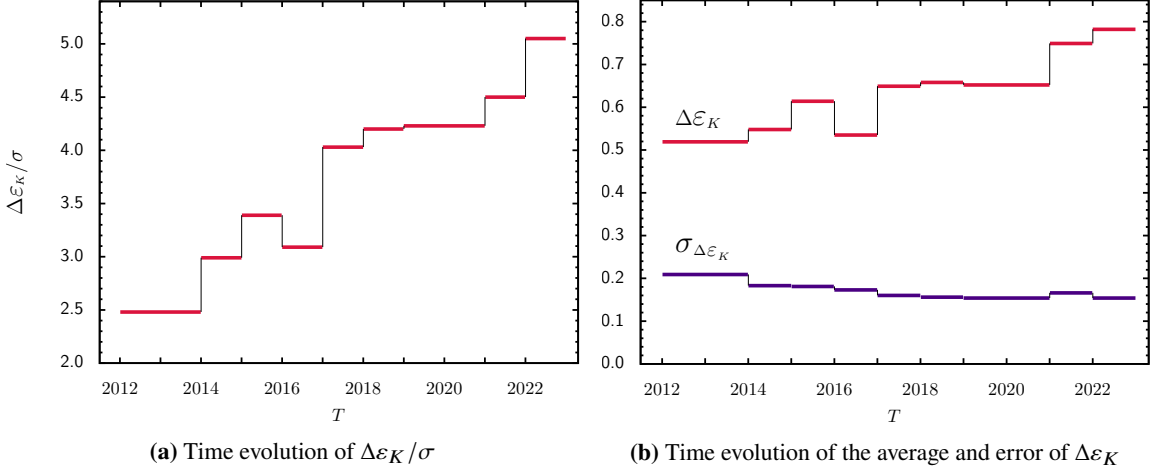


Figure 2: Time history of (a) $\Delta\varepsilon_K/\sigma$, and (b) $\Delta\varepsilon_K$ and $\sigma_{\Delta\varepsilon_K}$.

show the time evolution of the average $\Delta\varepsilon_K$ and the error $\sigma_{\Delta\varepsilon_K}$ during the period of 2012–2022.

At present, we find that the largest error ($\approx 50\%$) in $|\varepsilon_K|^{\text{SM}}$ comes from $|V_{cb}|$.² Hence, it is essential to reduce the errors in $|V_{cb}|$ as much as possible. To achieve this goal, there is an on-going project to extract exclusive $|V_{cb}|$ using the Oktay-Kronfeld (OK) action for the heavy quarks to calculate the form factors for $\bar{B} \rightarrow D^{(*)}\ell\bar{\nu}$ decays [38–44].

A large portion of interesting results for $|\varepsilon_K|^{\text{SM}}$ and $\Delta\varepsilon_K$ could not be presented in Table 8 and in Fig. 2 due to lack of space: for example, results for $|\varepsilon_K|^{\text{SM}}$ obtained using exclusive $|V_{cb}|$ (FLAG 2021), results for $|\varepsilon_K|^{\text{SM}}$ obtained using ξ_0 determined by the direct method, and so on. We plan to report them collectively in Ref. [45].

Acknowledgments

We thank Jon Bailey, Yong-Chull Jang, Stephen Sharpe, and Rajan Gupta for helpful discussion. We thank Guido Martinelli for providing us the most updated results of the UTfit Collaboration in time. The research of W. Lee is supported by the Mid-Career Research Program (Grant No. NRF-2019R1A2C2085685) of the NRF grant funded by the Korean government (MSIT). W. Lee would like to acknowledge the support from the KISTI supercomputing center through the strategic support program for the supercomputing application research (No. KSC-2018-CHA-0043, KSC-2020-CHA-0001). Computations were carried out in part on the DAVID cluster at Seoul National University.

References

[1] **SWME** Collaboration, W. Lee, J. Kim, Y.-C. Jang, S. Lee, J. Leem, C. Park, and S. Park, *2021 update on ε_K with lattice QCD inputs*, *PoS LATTICE2021* (2021) 078, [[2202.11473](#)].

BABAR experimental results.

²Refer to Table 6 (b) for more details.

- [2] **LANL-SWME** Collaboration, J. Kim, S. Lee, W. Lee, Y.-C. Jang, J. Leem, and S. Park *PoS LATTICE2019* (2019) 029, [[1912.03024](#)].
- [3] J. A. Bailey *et al.* *Phys. Rev.* **D98** (2018) 094505, [[1808.09657](#)].
- [4] J. A. Bailey, Y.-C. Jang, W. Lee, and S. Park *Phys. Rev.* **D92** (2015) 034510, [[1503.05388](#)].
- [5] J. A. Bailey *et al.* *PoS LATTICE2018* (2018) 284, [[1810.09761](#)].
- [6] Y.-C. Jang, W. Lee, S. Lee, and J. Leem *EPJ Web Conf.* **175** (2018) 14015, [[1710.06614](#)].
- [7] J. A. Bailey, Y.-C. Jang, W. Lee, and S. Park *PoS LATTICE2015* (2015) 348, [[1511.00969](#)].
- [8] **Flavour Lattice Averaging Group (FLAG)** Collaboration, Y. Aoki *et al.* *Eur. Phys. J. C* **82** (2022), no. 10 869, [[2111.09849](#)].
- [9] J. Charles *et al.* *Eur.Phys.J.* **C41** (2005) 1–131, [[hep-ph/0406184](#)]. updated results and plots available at: <http://ckmfitter.in2p3.fr>.
- [10] M. Bona *et al.* *JHEP* **10** (2006) 081, [[hep-ph/0606167](#)]. Standard Model fit results: Summer 2016 (ICHEP 2016): <http://www.utfit.org>.
- [11] **UTfit** Collaboration, M. Bona *et al.* [2212.03894](#).
- [12] A. J. Buras and D. Guadagnoli *Phys.Rev.* **D78** (2008) 033005, [[0805.3887](#)].
- [13] J. Brod and M. Gorbahn *Phys.Rev.* **D82** (2010) 094026, [[1007.0684](#)].
- [14] **Fermilab Lattice, MILC** Collaboration, A. Bazavov *et al.* *Eur. Phys. J. C* **82** (2022), no. 12 1141, [[2105.14019](#)].
- [15] A. Barone, A. Jüttner, S. Hashimoto, T. Kaneko, and R. Kellermann, *Inclusive semi-leptonic $B_{(s)}$ mesons decay at the physical b quark mass*, *PoS LATTICE2022* (2023) 403, [[2211.15623](#)].
- [16] **HFLAV** Collaboration, Y. S. Amhis *et al.* *Eur. Phys. J. C* **81** (2021), no. 3 226, [[1909.12524](#)].
- [17] **Belle** Collaboration, E. Waheed *et al.* *Phys. Rev. D* **100** (2019), no. 5 052007, [[1809.03290](#)]. [Erratum: *Phys.Rev.D* 103, 079901 (2021)].
- [18] **BaBar** Collaboration, J. P. Lees *et al.* *Phys. Rev. Lett.* **123** (2019), no. 9 091801, [[1903.10002](#)].
- [19] **LHCb** Collaboration, R. Aaij *et al.* *Phys. Rev. D* **101** (2020), no. 7 072004, [[2001.03225](#)].
- [20] M. Bordone, B. Capdevila, and P. Gambino *Phys. Lett. B* **822** (2021) 136679, [[2107.00604](#)].
- [21] P. Gambino, K. J. Healey, and S. Turczyk *Phys. Lett.* **B763** (2016) 60–65, [[1606.06174](#)].
- [22] T. Blum *et al.* *Phys. Rev.* **D91** (2015) 074502, [[1502.00263](#)].

- [23] Z. Bai *et al.* *Phys. Rev. Lett.* **115** (2015) 212001, [[1505.07863](#)].
- [24] **Particle Data Group** Collaboration, P. Zyla *et al.* *PTEP* **2020** (2020), no. 8 083C01.
- [25] **RBC, UKQCD** Collaboration, R. Abbott *et al.* *Phys. Rev. D* **102** (2020), no. 5 054509, [[2004.09440](#)].
- [26] B. J. Choi *et al.* *Phys. Rev.* **D93** (2016) 014511, [[1509.00592](#)].
- [27] T. Blum *et al.* *Phys. Rev.* **D93** (2016) 074505, [[1411.7017](#)].
- [28] J. Laiho and R. S. Van de Water *PoS LATTICE2011* (2011) 293, [[1112.4861](#)].
- [29] S. Durr *et al.* *Phys. Lett.* **B705** (2011) 477–481, [[1106.3230](#)].
- [30] **Particle Data Group** Collaboration, R. L. Workman and Others *PTEP* **2022** (2022) 083C01.
- [31] A. J. Buras, D. Guadagnoli, and G. Isidori *Phys.Lett.* **B688** (2010) 309–313, [[1002.3612](#)].
- [32] N. Christ *et al.* *Phys.Rev.* **D88** (2013) 014508, [[1212.5931](#)].
- [33] N. Christ *et al.* *PoS LATTICE2013* (2014) 397, [[1402.2577](#)].
- [34] J. Brod, M. Gorbahn, and E. Stamou *Phys. Rev. Lett.* **125** (2020), no. 17 171803, [[1911.06822](#)].
- [35] M. Tanabashi *et al.* *Phys. Rev.* **D98** (2018) 030001. <http://pdg.lbl.gov/2019/>.
- [36] **CDF** Collaboration, T. Aaltonen *et al.* *Science* **376** (2022), no. 6589 170–176.
- [37] C. Patrignani *et al.* *Chin. Phys.* **C40** (2016) 100001. <https://pdg.lbl.gov/>.
- [38] T. Bhattacharya, B. J. Choi, R. Gupta, Y.-C. Jang, S. Jwa, S. Lee, W. Lee, J. Leem, S. Park, and B. Yoon *PoS LATTICE2021* (2021) 136, [[2204.05848](#)].
- [39] **LANL-SWME** Collaboration, S. Park, T. Bhattacharya, R. Gupta, Y.-C. Jang, B. J. Choi, S. Jwa, S. Lee, W. Lee, and J. Leem *PoS LATTICE2019* (2020) 050, [[2002.04755](#)].
- [40] **LANL/SWME** Collaboration, T. Bhattacharya, B. J. Choi, R. Gupta, Y.-C. Jang, S. Jwa, S. Lee, W. Lee, J. Leem, and S. Park *PoS LATTICE2019* (2020) 056, [[2003.09206](#)].
- [41] T. Bhattacharya *et al.* *PoS LATTICE2018* (2018) 283, [[1812.07675](#)].
- [42] J. A. Bailey *et al.* *EPJ Web Conf.* **175** (2018) 13012, [[1711.01786](#)].
- [43] J. Bailey, Y.-C. Jang, W. Lee, and J. Leem *EPJ Web Conf.* **175** (2018) 14010, [[1711.01777](#)].
- [44] **LANL-SWME** Collaboration, J. A. Bailey, Y.-C. Jang, S. Lee, W. Lee, and J. Leem *Phys. Rev. D* **105** (2022), no. 3 034509, [[2001.05590](#)].
- [45] **SWME** Collaboration, J. Bailey, J. Kim, S. Lee, W. Lee, Y.-C. Jang, J. Leem, S. Park, *et al.* in preparation.